Laser Wakefield Acceleration of Electrons at Ecole Polytechnique

Presented by D. Bernard

F. Amiranoff[1], S. Baton[1], D. Bernard[2], B. Cros[3], D. Descamps[1], F. Dorchies[1], F. Jacquet[2], V. Malka[1], J. R. Marquès[1], G. Matthieussent[3], P. Miné[2], A. Modena[1], P. Mora[4], J. Morillo[5], Z. Najmudin[6]

[1] *Laboratoire pour l'Utilisation des Lasers Intenses, Ecole Polytechnique, CNRS, 91128 Palaiseau, France*

[2] *Laboratoire de Physique Nucléaire et des Hautes Energies, Ecole Polytechnique, IN2P3 & CNRS, 91128 Palaiseau, France*

[3] *Laboratoire de Physique des Gaz et des Plasmas, CNRS, Université Paris Sud, 91405 Orsay, France*

[4] *Centre de Physique Théorique, Ecole Polytechnique, CNRS, 91128 Palaiseau, France*

[5] *Laboratoire des Solides Irradiés, CEA/DSM/DRECAM,URA-CNRS 1380, Ecole Polytechnique, 91128 Palaiseau, France*

[6] *Imperial College, Blackett Laboratory, SW7 2AZ London, UK*

Abstract. The acceleration of electrons injected in a plasma wave generated by the laser wakefield mechanism has been observed. A maximum energy gain of 1.6 MeV has been measured and the maximum longitudinal electric field is estimated to 1.5 GV/m. The experimental data agree with theoretical predictions when 3D effects are taken into account. The duration of the plasma wave inferred from the number of accelerated electrons is of the order of 1 ps.

I INTRODUCTION

The generation of large amplitude electric fields in plasmas by high-power lasers has been studied for several years in the context of high-field particle acceleration [1]. The ponderomotive force of the laser excites a longitudinal electron plasma wave (EPW) with a phase velocity close to the speed of light [2]. Two mechanisms have been considered to excite the EPW.

In the Laser Beat Wave Acceleration (LBWA) approach, the beating of a two frequency laser creates a modulation of its intensity. When the frequency difference is equal to the natural oscillation frequency of the plasma electrons ω_p, an EPW is excited resonantly. This can lead to large amplitude electric fields. A precise tuning of the electron density is therefore mandatory in LBWA experiments. LBWA has been extensively studied during the 90's with 1 μm [3] and 10 μm [4–6] lasers.

In the "standard" Laser Wake Field Acceleration (LWFA) approach, a single short laser pulse excites the EPW [2,7,8]. As the ponderomotive force associated with the longitudinal gradient of the laser intensity exerts two successive pushes in opposite directions on the plasma electrons, the excitation of the EPW is maximum when the laser pulse duration is of the order of $1/\omega_p$.

At high electron density, and high laser intensity, a long — with respect to $1/\omega_p$ — laser pulse breaks into short pulselets at $1/\omega_p$ through the stimulated Raman scattering instability [9–11]. In this self-modulated mode (SM LWFA), the very high longitudinal electric field of the EPW traps plasma electrons and accelerates them to high energies [12–16]. However, SM LWFA may not be the best candidate for very high energy accelerators, in particular because the EPW grows from an instability so that its phase is unpredictable, and also because of the low Lorentz factor $\gamma_p \approx \omega/\omega_p$ of the phase velocity of the EPW at high electron density.

Standard LWFA seems particularly suited for particle acceleration. It is not affected by saturation (e.g. relativistic detuning [5] or modulational instability [3]) as is LBWA, and operates at low density, where γ_p can be quite high. The excitation of radial EPW by laser wake field has already been observed by two-pulse frequency-domain interferometry [17,18].

We present the first observation of LWFA of injected electrons. Part of the material presented here will be published elsewhere [19]. A particular emphasis has been given to the separation of the signal from the background (BG) noise in the design of the experimental apparatus [23] and in the analysis of the data. In the case of LBWA experiments, Clayton *et al.* have shown that magnetic and/or transverse electric fields, due to a Weibel-like instability [20], still exist in the plasma a long (a few nanoseconds) time after the excitation of the EPW. Electrons deflected by such fields can scatter on the walls of the vacuum chamber and provide spurious signal, as is possibly the case in [21] and in the surprising result of [22].

II LASER WAKEFIELD ACCELERATION

The transverse and longitudinal components of a linear EPW created by laser wakefield, for a laser beam with a gaussian radial profile and a gaussian time distribution, can be expressed [1,7] as : $E_r = (4r/w^2)A\sin(\omega_p t - k_p z)$ and $E_z = k_p A\cos(\omega_p t - k_p z)$, with

$$A = \sqrt{\pi}\omega_p\tau_0 \exp(-\frac{\omega_p^2\tau_0^2}{4})\frac{I_{max}e}{2\epsilon_0 mc\omega^2}\exp(-\frac{2r^2}{w^2}), \qquad (1)$$

where the time variation of the laser intensity is described by $\exp(-(t/\tau_0)^2)$, I_{max} is the maximum intensity, w the $1/e^2$ radius in intensity, and $k_p = \omega_p/c$. At a given value of τ_0, E_z varies like $(\omega_p\tau_0)^2\exp(-(\omega_p\tau_0)^2/4)$. This gives a broad maximum close to $\omega_p\tau_0 = 2$, i.e. $\omega_p\tau = 4\sqrt{\ln 2}$, where τ is the pulse duration at FWHM. With $\tau = 400$ fs, this corresponds to an electron density $n = 2.2\ 10^{16}\mathrm{cm}^{-3}$, an EPW wavelength $\lambda_p = 226\ \mu$m, and an EPW Lorentz factor $\gamma_p = 214$. The corresponding Helium pressure is 0.4 mbar for a fully ionized plasma. Finally, the maximum electric field at resonance is $E_z[\mathrm{GV/m}]=1.35\ 10^{-18}I_{max}[\mathrm{W/cm^2}](\lambda[\mu\mathrm{m}])^2/\tau[\mathrm{ps}]$. The relative longitudinal perturbation of the electron density is $\delta_{||} = E_z/E_0$, where $E_0 = mc\omega_p/e$.

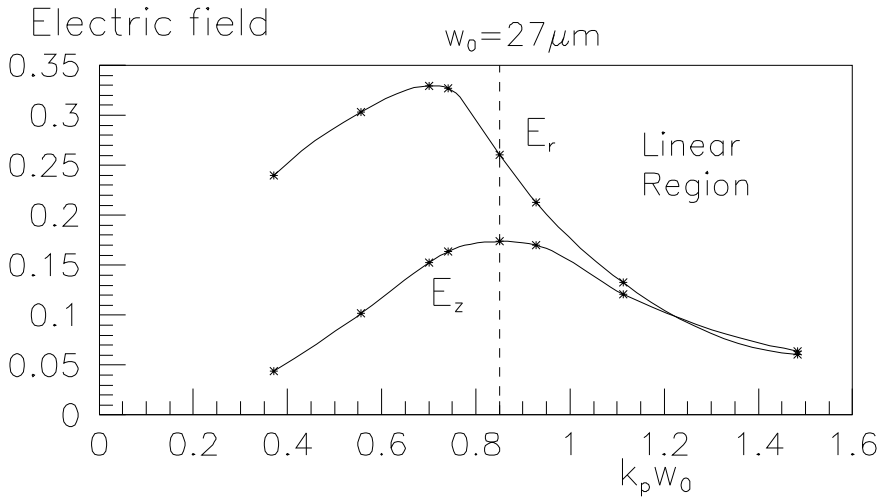

FIGURE 1. Variation of the longitudinal (E_z) and transverse (E_r) electric field in units of the cold wave breaking limit E_0, as a function of the laser spot size w in units of $2\pi/\lambda_p$. The laser energy is 3 J, duration 350 fs, and $\omega_p\tau_0 = 2$ (E_0=16 GV/m). The limit of the linear region is obtained for $\delta_\perp \approx 2$, (dashed line), and is approximately independent of laser energy.

The ratio of the transverse to the longitudinal electric field, at $r \approx w_0/\sqrt{2}$ is $E_r/E_z = \sqrt{2}\lambda_p/\pi w_0$, here equal to 4, w_0 being the laser beam size w at the waist. We obtain the value of the relative transverse perturbation of the electron density [17] by $\delta_\perp/\delta_{||} = (E_r/E_z)^2$, here equal to 16. This means that, in our conditions,

the EPW is mainly excited in the radial regime : the transverse electric field is stronger than the longitudinal electric field.

Particle simulations using the model described in Ref. [24] show (Fig. 1) that with our parameters, E_z is actually lower than the linear value given above, when the laser energy is so high that $\delta_\perp \geq 2$. The cavitation created by the radial oscillation affects the development of the longitudinal oscillation. The corresponding limit value of $\delta_{||}$ is here $\approx 10 - 20\%$.

III EXPERIMENTAL APPARATUS

The experimental apparatus is based on the existing facility already used for the study of LBWA [3], and is presented in Ref. [23]. A sketch of the present experiment can be found in Fig. 2. We use the 400 fs, 1.057 μm chirped pulse amplification laser at LULI. The 80 mm diameter beam is injected into a pulse compressor, and

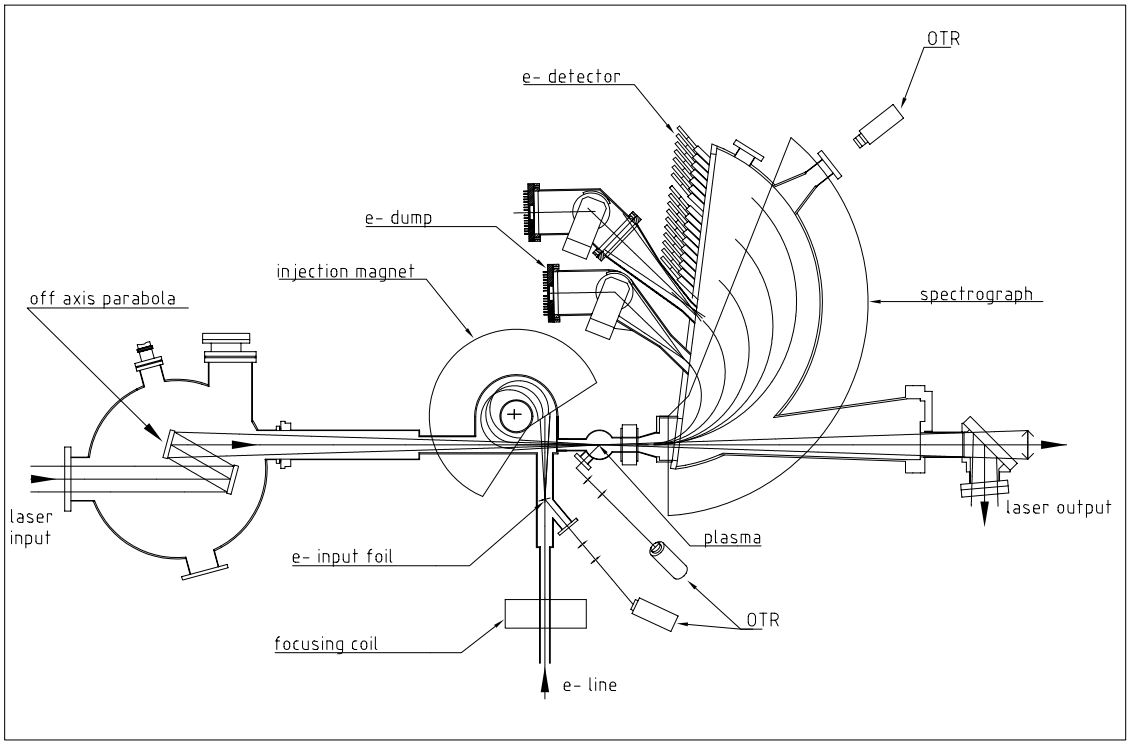

FIGURE 2. Layout of the experiment. See text and Ref. [23].

focused in a gas filled chamber by a 1.4 m focal length 30° off-axis parabola. A fraction of the compressed beam is collected before focusing and sent to a single-shot second-order autocorrelator for pulse duration measurement. A low intensity fraction of the beam is collected after the plasma and sent to a focal spot monitor. A 300 μA cw electron beam is injected in the plasma at a total energy of 3 MeV

with an RMS spot size of 30μm and an RMS divergence of 10 mrad [23]. The accelerated electrons are measured by a magnetic spectrograph and 17 detectors in the range 3.3 to 5.9 MeV. The linear gates have been withdrawn, and the voltage of the photomultipliers was tuned so that the calibration factor was equal to 2.5 ADC (analog to digital converter) count per electron. The duration of the gate was set to 20 ns.

IV EXPERIMENTAL RESULTS

A series of 250 shots has been performed, most of them with a laser energy in the range 4–9 J. On average, after compression, 20% of this energy is focused to a spot with typical size $w_{0,H} = 30$ μm (horizontal waist) and $w_{0,V} = 19$ μm (vertical waist), with Rayleigh length of $z_{0,H} = 2.3$ mm and $z_{0,V} = 2.0$ mm. With a central spot energy of 1.5 J, the values of the maximum power, intensity, electric field, EPW amplitude, and of the expected linear energy gain are P_{max}=3.5 TW, $I_{max} = 4 \cdot 10^{17}$W/cm^2, E_z=1.5 GV/m, $\delta_{\|}$=10%, $\Delta W = \pi e z_0 E_z$=10 MeV. The main source of fluctuation is due to the laser pulse duration. For shots for which the quantities τ, E, $w_{0,H,V}$ could be measured, the amplitude varies in the range $\delta_{\|}$=1–15%. Electron acceleration was observed in all of these shots.

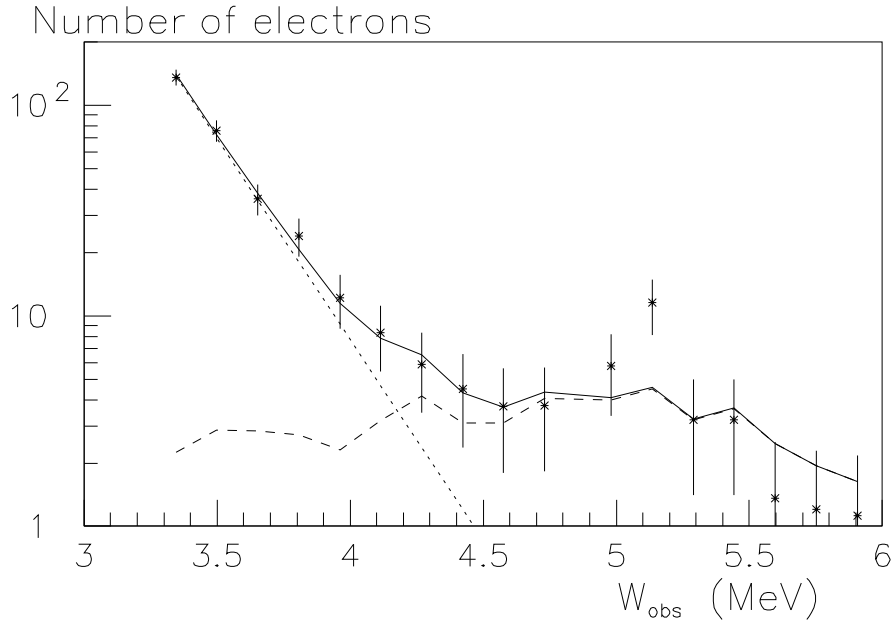

FIGURE 3. Spectrum of a typical shot (dots). The fit is described in the text. The continuous line shows the sum of the two contributions.

A typical spectrum is presented in Fig. 3 (dots). It shows a peak at low electron energy, that can be fitted by a decreasing exponential (dotted line) and a high

energy tail (dashed line) that has the same shape as the BG noise spectrum, as explained below.

To check the energy of the electrons impinging on a given channel, we have inserted stainless steel filters with various thicknesses in front of some scintillators. The signal of the corresponding channel is reduced by a factor which depends on the mean electron energy. The transmission factor for laser shots and BG noise runs is compared with the result of a simulation [25] at the electron energy corresponding to the channel (Fig. 4). From the low transmission factor in channel 12, with

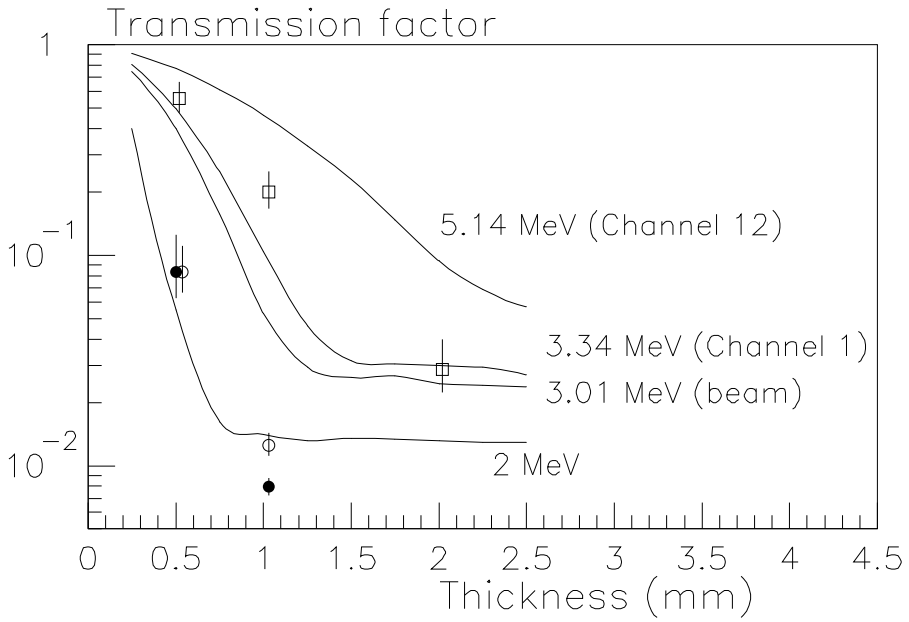

FIGURE 4. Transmission factors with stainless steel filters as a function of their thickness; channel 1 : □ (laser shots); channel 12 : ○ (laser shots), ● (gas BG noise runs). The error bars indicate the dispersion on several shots or runs. Continuous lines : simulation [25].

nominal electron energy of 5.14 MeV, we infer that the high energy tail is actually due to electrons with an average energy of about 2 MeV.

We now examine the various contributions to the BG noise. The BG noise due to Coulomb scattering of the beam electrons in the gas, has been substracted in Fig. 3. This noise has been studied in separate runs, without the laser. For each channel, the average value scales with pressure with a typical proportionality factor of 8 e^-/mbar. This factor does not decrease with the channel number as for simple Coulomb scattering. This "gas" BG is due to electrons deflected at low angle in the gas, that impact on the flange of the bottle neck of the dump. Part of these are back-scattered, re-enter the magnetic field of the spectrograph, and may fly back into the detector [23].

The tail in Fig. 3 is due to an excess of BG noise. It is observed only for shots with accelerated electrons, i.e. *in correlation with the EPW*. We call it "EPW"

BG noise. It is due to electrons deflected in the plasma close to the waist, while Coulomb scattering occurs along the whole path of the electrons, with a different geometry. To simulate the former, we have introduced a 11 μm Al foil at focus, in vacuum. The obtained noise spectrum has a shape similar to the shape of the gas spectrum. The electrons scattered at large angle in the foil are blocked by the d_1 collimator (See Fig. 12 of Ref. [23]). Few of them are re-scattered at the edge of the collimator. As the latter is not at focus, some of them impact on the flange of the dump. This is the reason for the similar shape of the two distributions.

The signals of three channels have also been recorded on a storage oscilloscope for each shot. A peak, about 10 ns in duration at 10%, is observed in correlation with the ADC recording, for channels 1 (signal), 8 and 12 (EPW BG noise). Therefore both the EPW BG noise and the signal are shorter than 10 ns, while the gas BG noise is obviously continuous. The EPW BG noise level is too high to be due only to the electrons deflected by the transverse electric field of the EPW, because of its short (ps) life-time, and because of the high rejection power of the collimation system [23], as shown by the low noise level induced by the foil. An effect like the Weibel instability already observed in ref. [20] is a good candidate to explain a long term (ns) deviation of the electrons. It could thus explain this BG. The signal is separated from the EPW BG noise by the process of the simultaneous fit of the exponential peak and of the tail (Fig. 3). We define the end point W_{obs} of the

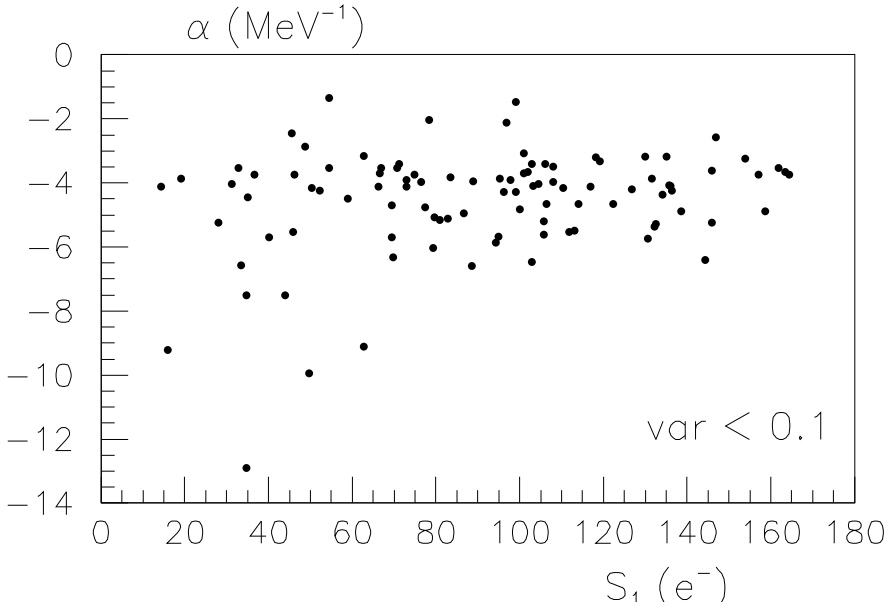

FIGURE 5. Variation of the slope α with the number of e^- in channel 1.

spectrum of the signal as the energy for which the exponential peak decreases to one electron. For the shots for which enough channels have a signal to make a fit, the slope α is found equal to $\alpha_0 = -4.4 \pm 1.1$ MeV^{-1}, a number that is observed

not to depend on the parameters of the laser pulse or of the plasma (as an example, the variation of α with the number of e^- in channel 1 is given in Fig. 5). Therefore we have used the same value $\alpha = \alpha_0$ to compute ΔW_{obs} for all the shots.

The variation of the signal S_1 in channel 1 with $\omega_p\tau_0$ is presented in fig. 6(left), where both ω_p and τ_0 have been varied. As expected, the data show a maximum close to $\omega_p\tau_0 = 2$. The spectrum of ΔW_{obs} is much broader (right), as ΔW_{obs} varies like $\log S_1$ in the exponential peak. Here, $\delta_{||}$ is low, and the length of the high gradient region, of the order of $2z_0$, is smaller than the dephasing length of the electrons with respect to the EPW, equal to 8 mm. Therefore, ΔW_{obs} should have the same resonant dependance with $\omega_p\tau_0$ as A (Eq. 1, and curve in Fig. 6 right). Note also that the maximum value of ΔW_{obs}, close to 1.6 MeV, is smaller than the value obtained from the linear approximation in 1D geometry, close to 10 MeV.

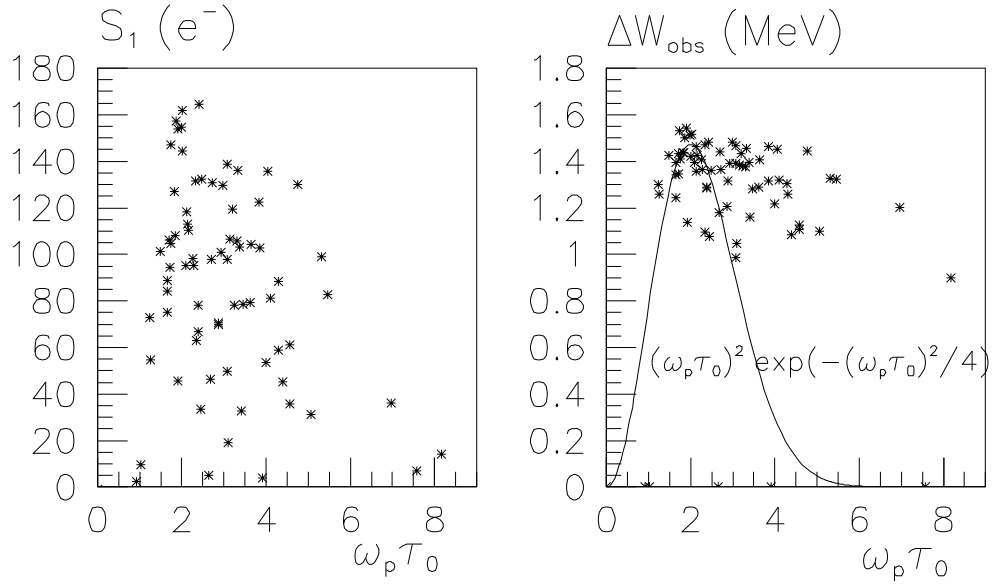

FIGURE 6. Variations of S_1(left) and of ΔW_{obs} (right) with $\omega_p\tau_0$. The fitting procedure ($S_1 > 10$ e^-) introduces a cut off at ΔW_{obs}=0.85 MeV. The pressure is varied in the range 0–2 mbar with half of the data taken at "resonance". The main source of variation of $\omega_p\tau_0$ is the fluctuation of τ_0. Only data with $\tau < 1$ ps are used. The curve describes the $\omega_p\tau_0$ dependence of E_z in linear LWFA theory.

The transverse electric field of the EPW affects the trajectories of the electrons. Depending on their phase, electrons undergo a focusing or defocusing force when they enter the EPW. The defocused electrons are expelled radially before they enter the high accelerating region. On the contrary, the focused electrons are transversely trapped in the EPW, and should be accelerated in it efficiently [26].

In fact, a numerical tracking of the trajectories of electrons in the EPW, using the code described in [27], shows that most of them miss the waist transversely.

This can be understood in the simple model of ref. [26], where the trajectory of an electron is described by a three domain approximation : a drift in free space, an "adiabatic" region where the electron is trapped by the transverse field, and another drift on exit. Trapping occurs very far from the waist, at a location where $\delta_{||}$ is equal to a critical value $\delta_c = \gamma(w_0/z_0)^2/4$ [26], here equal to 10^{-3}, γ being the electron Lorentz factor. Then, in the central region, the evolution of the envelope of the electron beam is determined by the evolution of the betatron function in the EPW, so that the beam size at the waist is $\sigma_w = \sigma_0 \sqrt[4]{\delta_{||}/\delta_c} z_0/\beta^*$ where σ_0 and β^* are the beam size and the betatron function at the waist in vacuum. For $\sigma_0 = 30\mu$m and $z_0 \approx \beta^*$, and for $\delta_{||} = 10\%$, we have $\sigma_w = 90\mu$m, much larger than the size of the plasma wave $\sigma_{\rm EPW} = w_0/2 \approx 10\mu$m. The key point is that after trapping in the EPW, the e^- beam size varies like $\sqrt{\beta} \propto \delta_{||}^{-1/4} \propto [1 + (z/z_0)^2]^{1/4}$, while in vacuum it varies like $w \propto [1 + (z/z_0)^2]^{1/2}$.

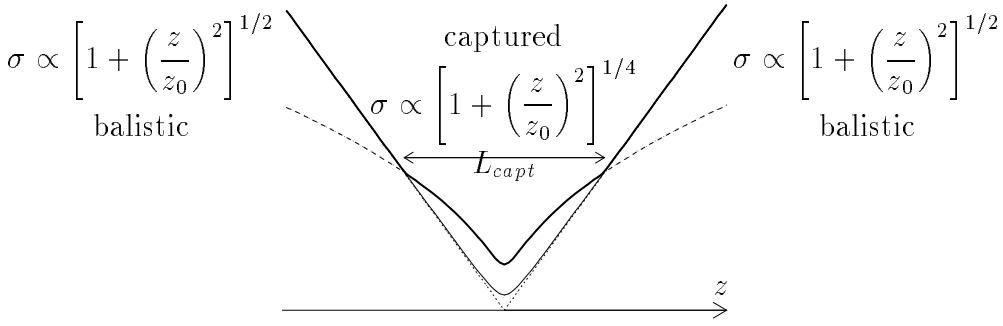

FIGURE 7. Scheme of the enveloppe of the electron beam (solid thick line). Solid thin line : balistic beam, dashed line : captured beam.

In the presence of the EPW, the decrease of the beam size while approaching the waist is much slower. A more precise description of this effect (Fig. 8, left) is obtained using the simulation; electrons are tracked [27] through an EPW computed in the linear regime, created by a laser beam, in the gaussian approximation with cylindrical symmetry, ie. according to eq. 1. Electrons injected on axis (curve a) undergo an acceleration or a deceleration, depending on their injection phase φ. Electrons injected with a tiny emittance (b) in the focusing part of the wave are not affected, while those that are defocused are expelled before the high accelerating gradient region is reached. Electrons injected with real emittance (c) miss the EPW waist even in the focusing part of the EPW. Note also that both the length of the completely ionized plasma, $L_{pl} \approx 25$ mm, and the length on which the electrons are captured by the EPW [26] $L_{capt} = 2z_0\sqrt{\delta/\delta_c} \approx 40$ mm, are larger than the dephasing length $L_{dephas} \approx 8$ mm : most of the electrons have the occasion to be expelled from the EPW by a defocusing field during their path through the EPW.

The corresponding fraction of the electrons accelerated throughout the plasma is low (Fig. 8, right) and the maximum energy gain observed in the simulation is

much lower than the maximum possible energy gain $\Delta W = \pi e z_0 E_z$. The slope of the simulated spectrum is in agreement with the observed value. The accelerated electrons are contained in a divergence angle of ± 70 mrad, well inside the acceptance of the detector. To reach the maximum possible energy gain, the increase of the radial size of the accelerated electron beam could be overcome either by an injection at a higher energy, or by a limitation of the EPW length, by using a gas jet.

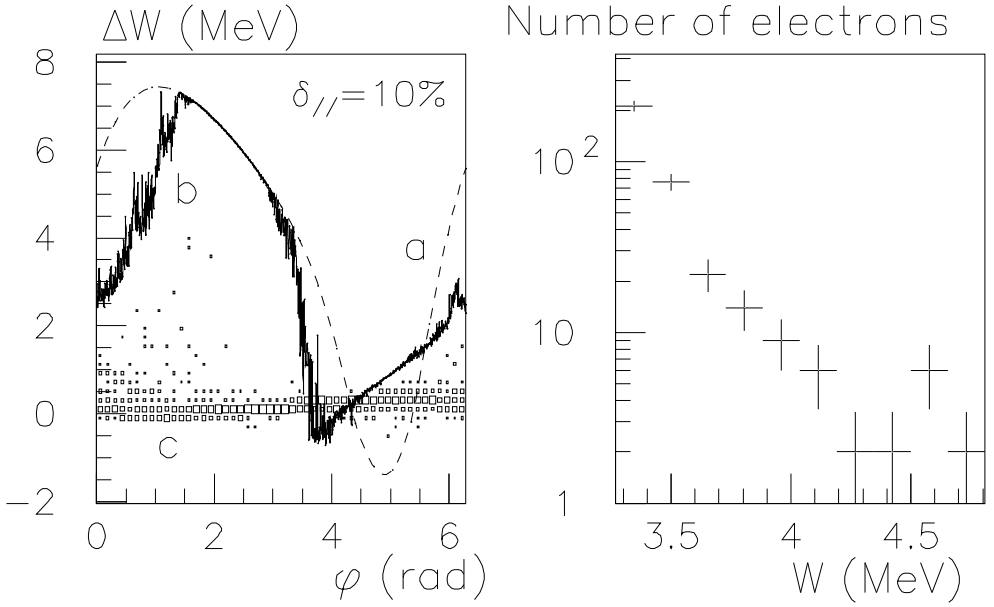

FIGURE 8. 3D MonteCarlo simulation [27] of the energy gain (left) of 1000 electrons as a function of their phase with respect to the EPW. a) beam on axis; b) small emittance beam (30 nm$\times$10 μrad RMS); c) real emittance beam (30 μm$\times$10 mrad RMS). The corresponding spectrum in the 10 first channels (right) shows an exponential peak with a slope of -6.1 MeV^{-1}.

Figure 9 shows electron spectra at three laser central energies. As the electron flow delivered by the Van de Graaf is constant during the life-time T of the EPW, we infer an estimate of T from a comparison of the normalisations of the observed and simulated spectra. The obtained value is of about 1 ps, in agreement with particle simulations using the model of Ref. [24].

V CONCLUSION

In conclusion, we have observed the acceleration of electrons injected in an EPW generated by laser wakefield, with a maximum energy gain of 1.6 MeV. We also observe a tail in the high energy channels. Our cross-check using stainless steel filters proves that this tail is actually due to low energy deflected electrons. This BG, clearly correlated with the plasma wave, can fake accelerated electrons in this

kind of experiments. The experimental data agree with theoretical predictions when 3D effects are taken into account.

VI ACKNOWLEDGEMENTS

We gratefully acknowledge the help of the technical staff of the LULI, LPNHE, LSI, and CEA/DSM/DAPNIA-SEA for this experiment. This work has been partially supported by Ecole Polytechnique, IN2P3-CNRS, SPI-CNRS, and by the EU Large Facility Program under Contract No. FMGE CT95 0044.

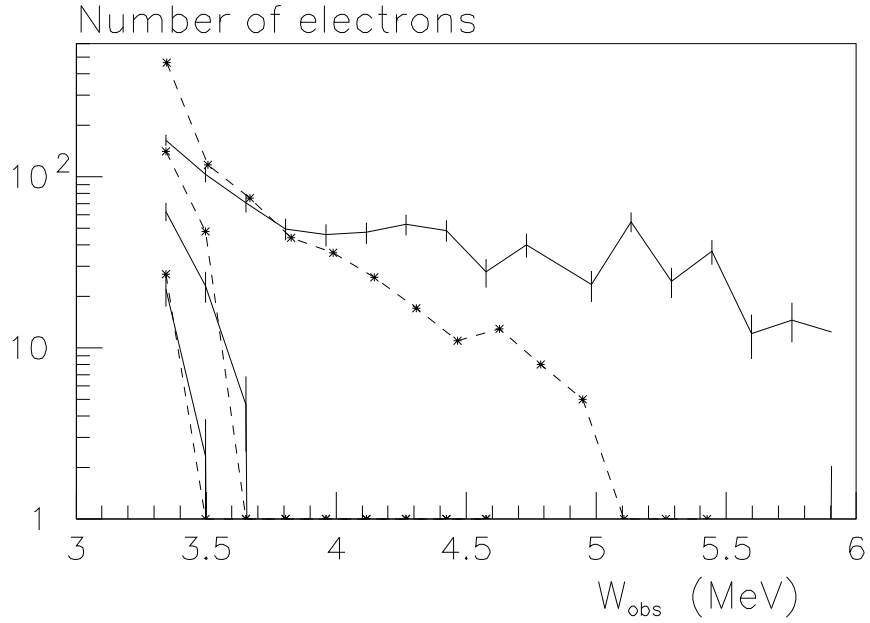

FIGURE 9. Electron spectra with $E = 0.25, 0.49, 2.1$ J (continuous lines) compared to simulated spectra (2000 incident electrons, dashed lines). At 2.1 J, the high energy tail is due to EPW BG noise.

REFERENCES

1. A review can be found in : E. Esarey *et al.*, IEEE Trans. Plasma Science, **24** 252 (1996).
2. T. Tajima and J. M. Dawson, Phys. Rev. Lett. **43**, 267 (1979).
3. F. Amiranoff *et al.*, Phys. Rev. Lett. **74**, 5220 (1995);
   F. Amiranoff *et al.*, IEEE Trans. on Plasma Sci., **24** 296 (1996).
4. Y. Kitagawa *et al.*, Phys. Rev. Lett. **68**, 48 (1992).
5. C. E. Clayton *et al.*, Phys. Rev. Lett. **70**, 37 (1993).
6. N. A. Ebrahim, J. Appl. Phys. **76**, 7645 (1994).
7. L. M. Gorbunov and V. I. Kirsanov, Zh. Eksp. Teor. Fiz. **93** 509 (1987); Sov. Phys. JETP **66** 290 (1987).
8. P. Sprangle *et al.*, Appl. Phys. Lett. **53** 2146 (1988).
9. N. E. Andreev *et al.*, Sov. Phys. JETP **55** 571 (1992).
10. T. M. Antonsen Jr. and P. Mora, Phys. Rev. Lett. **69** 2204 (1992).
11. P. Sprangle *et al.*, Phys. Rev. Lett. **69** 2200 (1992).
12. A. Modena *et al.*, Nature, **377** 606 (1995).
13. C. Coverdale *et al.*, Phys. Rev. Lett. **74** 4659 (1995).
14. K. Nakajima *et al.*, Phys. Rev. Lett. **74** 4428 (1995).
15. A. Ting *et al.*, Phys. Plasmas **5** 1889 (1997).
16. R. Wagner *et al.*, Phys. Rev. Lett. **78**, 3125 (1997)
17. J. R. Marquès *et al.*, Phys. Rev. Lett. **76** 3566 (1996);
    C. W. Siders *et al.*, Phys. Rev. Lett. **76** 3570 (1996).
18. J. R. Marquès *et al.*, Phys. Rev. Lett. **78** 3463 (1997).
19. Observation of Laser Wakefield Acceleration of Electrons, F. Amiranoff *et al.*, preprint X-LPNHE 98/02, April 1998, to appear in Phys. Rev. Lett.
20. C. E. Clayton *et al.*, Phys. Plasma, **1** 1753 (1994).
21. K. Nakajima *et al.*, in Proceedings of the International Workshop on Acceleration and Radiation Generation in Space and Laboratory Plasmas, Kardamily, Greece, 1993, Published in Phys.Scripta T52:61-64,1994.
22. M. Kando *et al.*, KEK Preprint 97-10, April 1997, submitted to Phys. Rev. Lett.
23. F. Amiranoff *et al.*, Nucl. Instr. and Meth. A **363** 497 (1995).
24. P. Mora, T. M. Antonsen Jr, Phys. Plasma **4** 217 (1997).
25. W. R. Nelson *et al.*, The EGS4 code system, SLAC report 265, Dec. 1985.
26. D. Bernard, in Proceedings of the 13th Advanced ICFA Beam Dynamics Workshop and 1st ICFA Novel and Advanced Accelerator Workshop, Kyoto, Japan, 1997, Nucl. Instrum. Methods Phys. Res. A 410 (1998) 418.
27. P. Mora, J. Appl. Phys. **71** 2087 (1992).